Human Molecular Genetics, 2012, Vol. 21, No. 17 **3845–3857**
doi:10.1093/hmg/dds213
Advance Access published on June 12, 2012

Loss of function of *Ifi202b* by a microdeletion on chromosome 1 of C57BL/6J mice suppresses *11β-hydroxysteroid dehydrogenase type 1* expression and development of obesity

Heike Vogel[1], Stephan Scherneck[1], Timo Kanzleiter[1], Verena Benz[1], Reinhart Kluge[1,2], Mandy Stadion[1], Sergiy Kryvych[1], Matthias Blüher[3], Nora Klöting[3], Hans-Georg Joost[2] and Annette Schürmann[1,*]

[1]Department of Experimental Diabetology and [2]Department of Pharmacology, German Institute of Human Nutrition Potsdam-Rehbruecke, Nuthetal, Germany, [3]Department of Medicine, University of Leipzig, Leipzig, Germany

Received April 18, 2012; Revised May 14, 2012; Accepted May 28, 2012

***Nob3* is a major obesity quantitative trait locus (QTL) identified in an intercross of New Zealand Obese (NZO) mice with C57BL/6J (B6), and by introgression of its 38 Mbp peak region into B6 (B6.NZO-*Nob3.38*). B6.NZO-*Nob3.38* mice carrying the NZO allele exhibited markedly increased body weight, fat mass, lean mass and a lower energy expenditure, than the corresponding B6 allele carriers. For positional cloning of the responsible obesity gene, five additional congenic lines (RCS) were generated and characterized, allowing to define a critical genomic interval comprising 43 genes. mRNA profiling and western blotting indicated that *Ifi202b*, a member of the *Ifi200* family of interferon inducible transcriptional modulators, was expressed in NZO-allele carriers but was undetectable in tissues of homozygous B6-allele carriers due to a microdeletion, including the first exon and the 5′-flanking region of *Ifi202b* in B6. Transcriptome analysis of adipose tissue of RCS revealed a marked induction of *11β-hydroxysteroid dehydrogenase type 1* (*11β-Hsd1*) expression in mice expressing *Ifi202b*. Furthermore, siRNA-mediated *Ifi202b* suppression in 3T3-L1 adipocytes resulted in a significant inhibition of *11β-Hsd1* expression, whereas an adenoviral-mediated overexpression of *Ifi202b* increased *11β-Hsd1* mRNA levels. Expression of human *IFI* orthologues was significantly increased in visceral adipose tissue of obese subjects. We suggest that the disruption of *Ifi202b* in B6 is responsible for the effects of the obesity QTL *Nob3*, and that *Ifi202b* modulates fat accumulation through expression of adipogenic genes such as *11β-Hsd1*.**

INTRODUCTION

Obesity is a complex disease based on the combination of multiple genes and their interaction with the environment (1,2). Genome-wide association studies have identified common single nucleotide polymorphisms (SNPs) associated with increased body mass index (BMI) such as *FTO*, *MC4R*, *BDNF* and *SH2B1* genes (3–6). However, together these polymorphisms account for a small percentage of the inherited variation in body weight indicating that a substantial proportion of the heritable component of the disease remains to be explained. Genetic linkage and association studies are additional approaches to associate gene loci with physiological traits like obesity. Numerous quantitative trait loci (QTL) reflecting broad genomic regions influencing body weight have been mapped but the identification of the individual gene(s) responsible for the phenotype remains difficult. Consequently, only a few percent of the many QTL that have been mapped resulted in the identification of the underlying gene (7).

The New Zealand Obese (NZO) mouse develops a polygenic disease pattern of obesity, insulin resistance and dyslipoproteinemia closely resembling the human metabolic syndrome

*To whom correspondence should be addressed at: German Institute of Human Nutrition, Arthur-Scheunert-Allee 114-116, D-14558 Nuthetal, Germany. Tel: +49 33200882368; Fax: +49 33200882334; Email: schuermann@dife.de

(8,9). In order to identify chromosomal segments associated with these traits, we performed genome-wide linkage analysis in a backcross population of the NZO and the Swiss Jim Lambert mouse and identified several QTL. By positional cloning, we have recently discovered two genes encoding the Rab-GAP protein TBC1D1 (10) and the transcription factor ZFP69 (11) that participate in the development of the metabolic syndrome. Furthermore, in an outcross population of NZO with the lean C57BL/6J (B6) mouse, we identified a major obesity QTL (*Nob3*) on distal mouse chromosome 1 (Chr. 1) with a LOD score of 16.1. This QTL is responsible for a difference in body weight of 13 g in week 22. Introgression of a 38 Mbp fragment (*Nob3.38*)—corresponding with the distal peak of the QTL—from NZO into the B6 background increased body weight significantly (12).

In the present study, we define a critical genomic interval of 2.2 Mbp within *Nob3.38* which influences body weight. We furthermore identify a B6-specific microdeletion disrupting expression of *Ifi202b* which modifies the expression of *11β-Hsd1* in adipose tissue, presumably protecting the B6 mouse from the development of severe obesity. We furthermore show that the corresponding human orthologues exhibit an altered expression in the visceral adipose tissue of obese subjects.

RESULTS

Identification of a critical region of *Nob3.38* with a series of recombinant congenic lines

Introgression of a 38 Mbp segment of the previously described QTL *Nob3* (12) from NZO into B6 (B6.NZO-*Nob3.38*; Fig. 1A) markedly increased body weight, fat mass and lean mass of male and female congenic mice kept on a high-fat diet (Fig. 1B). Histology of white adipose tissue indicated that adipocytes of NZO-allele carriers were much larger than those of the corresponding B6-allele carriers (Supplementary Material, Fig. S1). This effect was associated with elevated mRNA levels for leptin (B6.NZO-$Nob3.38^{N/N}$: 3.08 ± 0.6; B6.NZO-$Nob3.38^{B/B}$: 1.34 ± 0.32 relative expression; $P < 0.005$). Furthermore, energy expenditure (EE) was significantly reduced in carriers of the NZO allele (Fig. 1C, left panel), consistent with the previously described reduction in rectal body temperature of parental NZO mice (8) and the *Nob3.38* NZO-allele carriers (12) (B6.NZO-$Nob3.38^{N/N}$: $37.2 \pm 0.1^{\circ}C$; B6.NZO-$Nob3.38^{B/B}$: $37.6 \pm 0.1^{\circ}C$; $P < 0.005$). In contrast, locomotor activity and food intake did not differ between B6.NZO-$Nob3.38^{N/N}$ and B6.NZO-$Nob3.38^{B/B}$ mice (Fig. 1C, middle and right panels, respectively). Thus, the difference in adiposity mediated by *Nob3* is associated with an altered thermogenesis which could be responsible for decreased total EE.

In order to define a critical segment of *Nob3.38* by a conventional strategy of positional cloning, additional congenic lines carrying different segments of *Nob3.38* (Fig. 2A) were generated and characterized with regard to their increment of body weight. Segments IV to VI were adipogenic, whereas segments VII and VIII (Fig. 2B) failed to increase body weights. Thus, the critical interval of *Nob3.38* on Chr. 1 comprising the adipogenic allele was convincingly defined by the markers D1Mit522 and D1Mit403 between 175.3 and 177.6 Mbp (Fig. 1A). For further fine mapping, we used SNPs and defined the borders of the critical interval of 2.2 Mbp (Fig. 2C) flanked by *Cadm3* and *Rgs7*. The interval comprises 14 genes encoding olfactory receptors, 1 transfer RNA, 7 pseudogenes, 4 gene models and 17 annotated genes, 7 of which belong to the *Ifi200* cluster (*Ifi202b, Ifi203, Ifi204, Ifi205, Mnda, Mndal* and *Aim2*). In addition to the known *Ifi200* genes, four other genes (*Pydc4, Pyhin1, Pydc3, BC094916*) and four gene models (*EG240921, LOC623121, AI607873, EG666028*) within the critical interval exhibit a significant similarity to *Ifi200* genes, and comprise the N-terminal DAPIN/PYRIN motif and/or a HIN200 domain that characterizes the *Ifi* family. In order to identify the responsible gene variant, we (i) sequenced the area between 175.3 and 177.5 Mbp and (ii) performed array-based expression studies in adipose tissue of B6.NZO-$Nob3.38^{B/B}$ and B6.NZO-$Nob3.38^{N/N}$ mice.

Sequencing of the 2.2 Mbp identified a total of 262 SNPs in 29 genes, 96 of these SNPs resulted in amino acid exchanges in 23 genes (Supplementary Material, Table S1).

Expression profiling of the critical region

Expression profiling of RNA from white adipose tissue of B6.NZO-$Nob3.38^{B/B}$ and B6.NZO-$Nob3.38^{N/N}$ mice (Supplementary Material, Table S2) indicated that four genes within the critical fragment of *Nob3.38* exhibit an altered expression. Most strikingly, one of them, *Ifi202b,* appeared not to be expressed in B6.NZO-$Nob3.38^{B/B}$ mice. We next studied the expression of transcripts and gene models within the critical region by quantitative real-time–polymerase chain reaction (qRT–PCR) in more detail. As shown in Figure 3A, we could confirm that mRNA of *Ifi202b* was undetectable in tissues of B6.NZO-$Nob3.38^{B/B}$ mice but expressed in B6.NZO-$Nob3.38^{N/N}$ mice. Expression of most genes belonging to the *Ifi200* cluster (*Aim2*, *EG240921*, *Pyhin1*, *Pydc3*, *Mndal*, *Ifi203*, *Ifi205*) were significantly reduced in tissues of B6.NZO-$Nob3.38^{N/N}$ mice in comparison to carriers of the B6 allele (Fig. 3A, Supplementary Material, Fig. S2), whereas *Pydc4*, *AI607873* and *Ifi204* did not show differences. Because of the high homology between some transcripts of the *Ifi200* cluster, it was impossible to design a unique probe for *Mnda* which would not also amplify other *Ifi* mRNAs.

We next tested the expression of *Ifi202b* in several tissues of the two parental strains NZO and B6. Highest levels of mRNA were determined in subcutaneous white adipose tissue and skeletal muscle of NZO mice, lower levels in gonadal white adipose tissue, brown adipose tissue, pancreas, and liver of NZO mice. Like in B6.NZO-$Nob3.38^{B/B}$ mice, we failed to detect *Ifi202b* mRNA in these tissues of B6 mice (Fig. 3B). A search in the databases identified expressed sequence tags of *Ifi202b* in thymus, taste buds, mammary gland, skin and vagina from B6. Therefore, we confirmed by qRT–PCR that mRNA of *Ifi202b* is indeed detectable in taste buds of B6 mice (Fig. 3B). However, as is shown below (Fig. 4), this expression appears to be driven by a different promoter.

Antiserum against peptides corresponding with the Ifi202b sequence detected specific signals in lysates of liver, skeletal muscle and white adipose tissue of NZO mice, but no signal

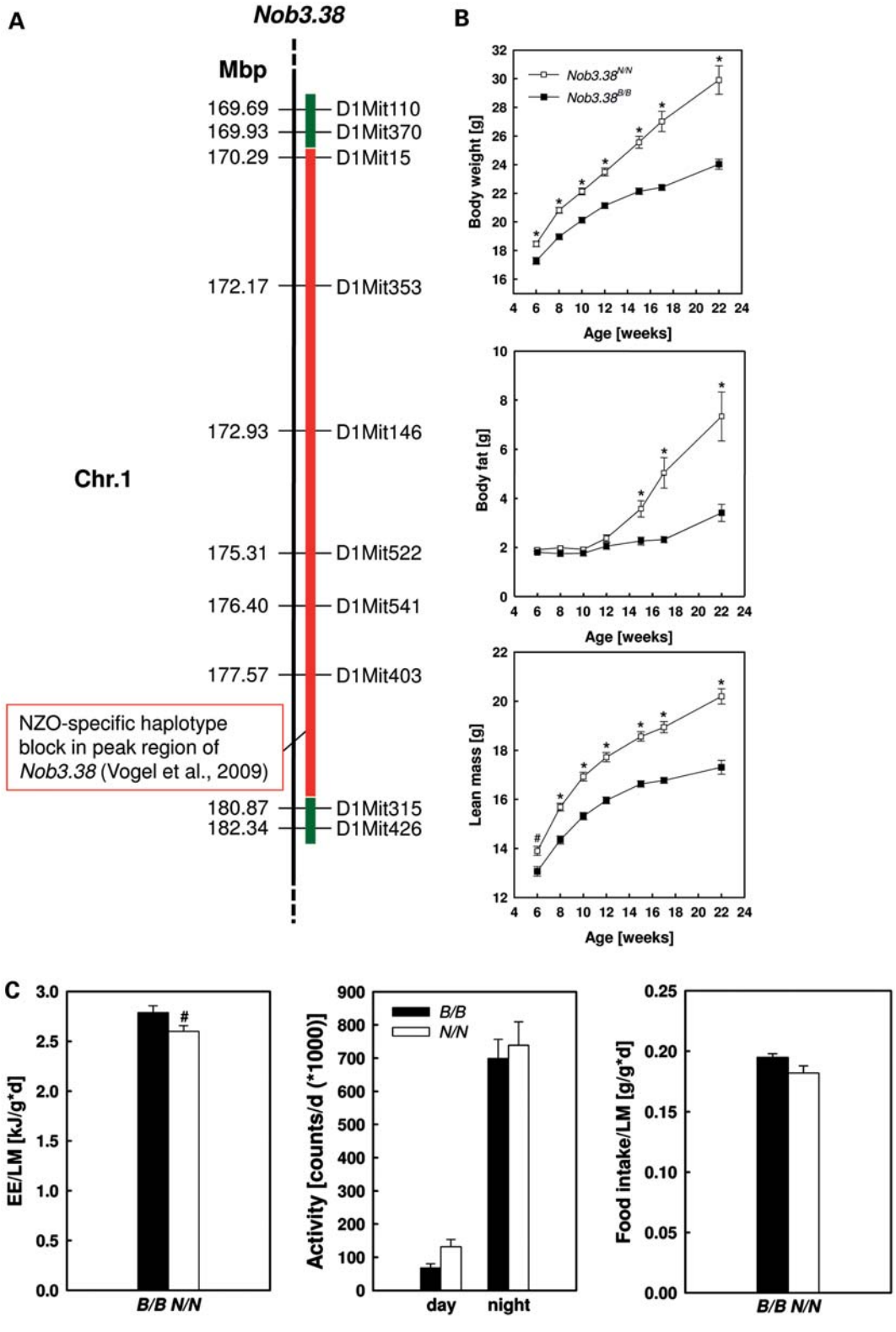

Figure 1. The peak region of the obesity QTL *Nob3* and phenotypic characterization of B6.NZO-*Nob3.38*$^{B/B}$ and B6.NZO-*Nob3.38*$^{N/N}$ mice. (**A**) The map depicts the polymorphic haplotype block (marked in red) of a comparison of NZO with B6 within the *Nob3.38* segment from NZO that was introgressed into C57BL/6J (green, non-polymorphic regions). A selection of microsatellite markers used for genotyping of B6.NZO-*Nob3.38* mice is indicated. (**B**) Development of body weight (upper panel), fat mass (middle panel) and lean mass (lower panel) of the two recombinant congenic lines that were kept on a HFD ($n = 22–32$). (**C**) EE (left panel) as determined over 24 h per g lean mass, locomotor activity in the home cage (middle panel) and food intake (right panel) of *B/B* and *N/N* mice on a HFD ($n = 13$). ($^{\#}P < 0.05$; $^{*}P < 0.001$).

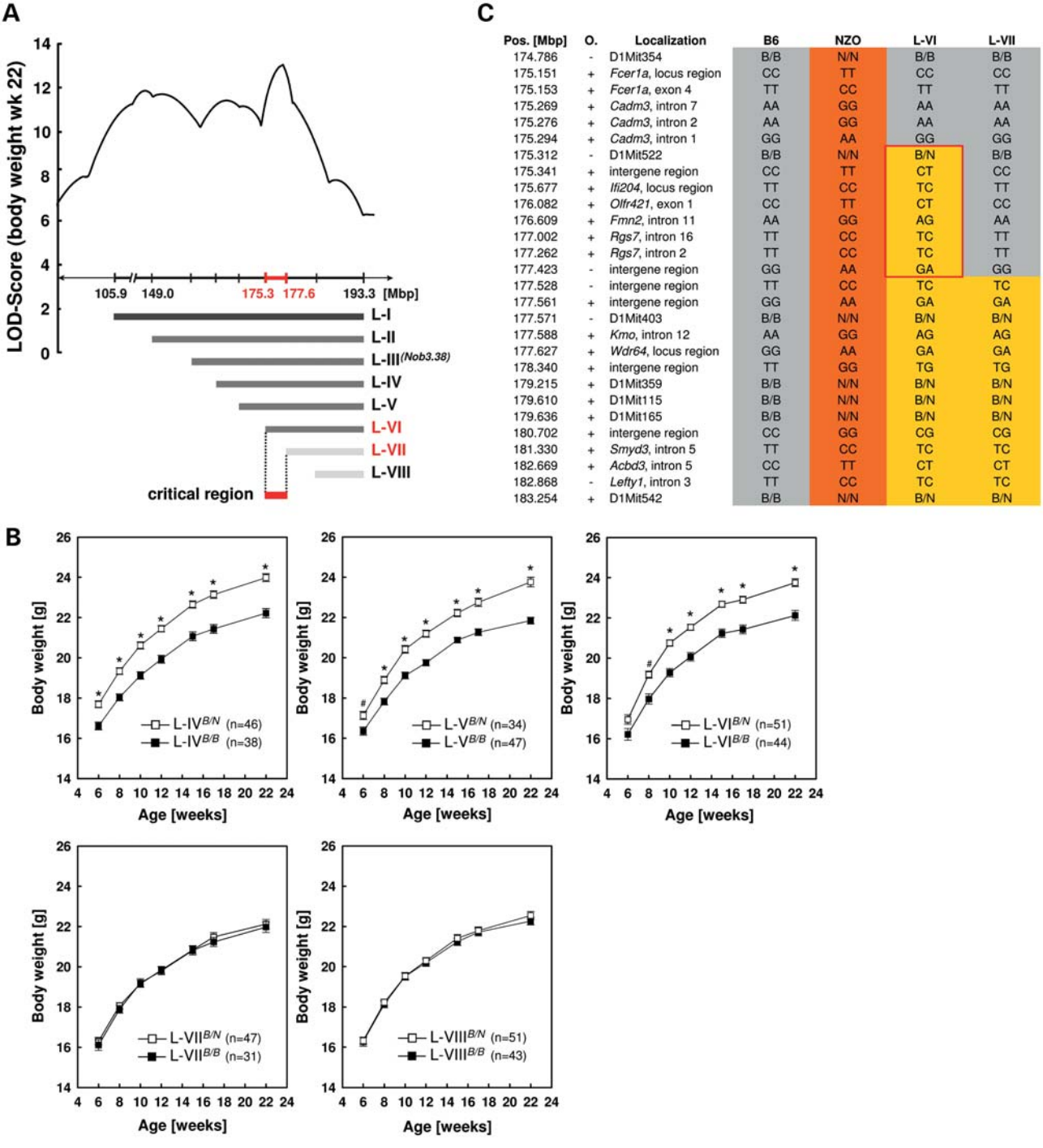

Figure 2. Identification of a minimal critical region of Chr. 1 affecting body weight. (**A**) Map of chromosomal fragments I–VIII of NZO introgressed into B6 background. (**B**) Body weight development (weeks 6–22) in female mice of recombinant congenic lines L–IV to L–VIII (N6 generation). The number of mice in each group is given in parenthesis. ($^{\#}P < 0.0005$; $^{*}P < 10^{-06}$). (**C**) Localization of SNPs and microsatellite markers used for fine mapping of the critical interval as defined by the congenic lines L–VI and L–VII. Yellow color depicts heterozygosity. The critical interval is highlighted by the red frame.

in tissues of B6 mice (Fig. 3C). In contrast to the qRT–PCR result, Ifi202b protein was considerably more abundant in the white adipose tissue (WAT) than in the other tissues. We next tested the expression of Ifi202b in tissues of B6.NZO-*Nob3.38*$^{B/B}$ and B6.NZO-*Nob3.38*$^{N/N}$ mice and could confirm the results obtained by qRT–PCR; Ifi202b protein is absent in skeletal muscle of B6-allele carriers but present in NZO-allele carriers (Fig. 3D).

In order to test whether the additive effect of *Nob3.38* on obesity corresponds with a similar effect of the locus on *Ifi202b* expression, we compared the *Ifi202b* expression in liver and white adipose tissue of heterozygous B6.NZO-

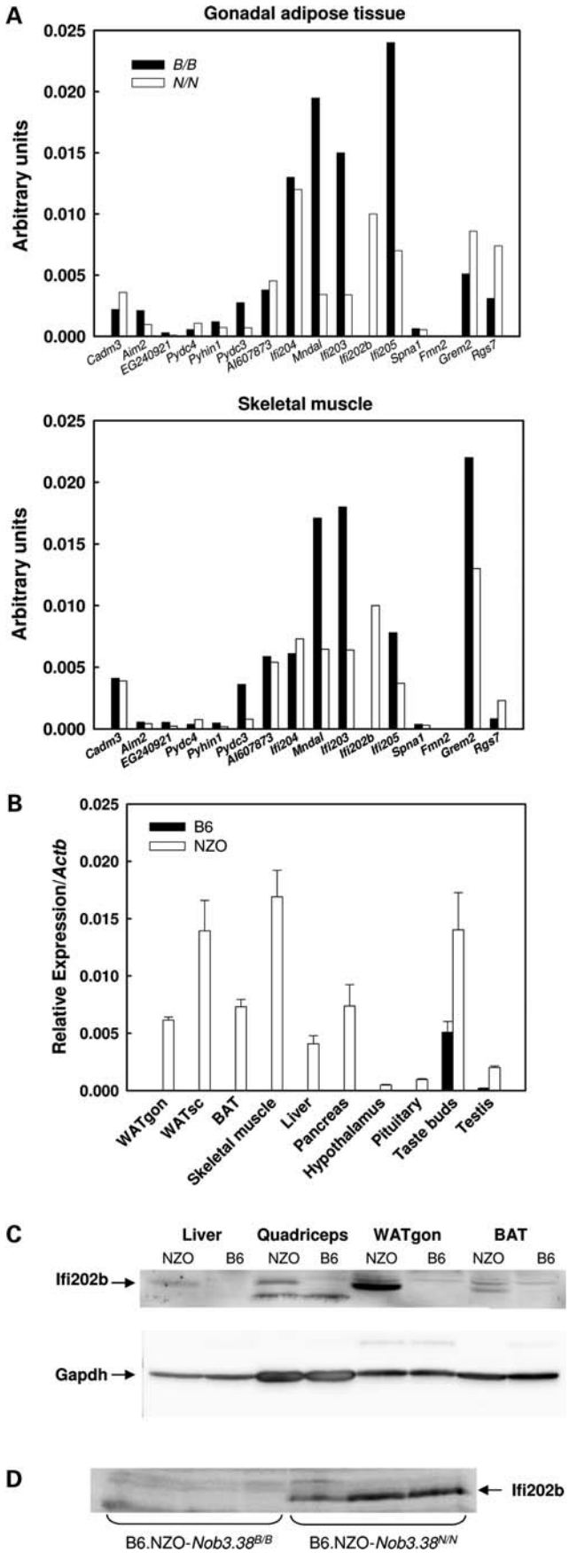

Nob3.38$^{B/N}$ and homozygous B6.NZO-*Nob3.38*$^{N/N}$ mice (Supplementary Material, Fig. S3). The *Ifi202b* mRNA levels are higher in homozygous *Nob3.38*$^{N/N}$ mice than in those carrying only one NZO allele (*Nob3.38*$^{N/B}$). We furthermore tested the body weight of heterozygous and homozygous mice and determined a dose-dependent effect (body weight of F2N5 mice in week 22: *B/B*: 23.7 $\pm$ 0.36 versus *N/B* 25.2 $\pm$ 0.34 with a difference of 1.5 g body weight; body weight of N6 mice in week 22: *B/B* 22.1 $\pm$ 0.19 versus *B/N* 23.2 $\pm$ 0.21 g with a difference of 1.1 g), indicating that *Nob3.38* exhibits a codominant effect on both body weight and *Ifi202b* gene expression.

Identification of a microdeletion disrupting the *Ifi202b* gene

In order to test the possibility that the striking difference in the *Ifi202b* expression between B6 and NZO allele carriers is the consequence of the formation of different mRNA species, we analysed the *Ifi202b* cDNA from taste buds (B6) and gonadal adipose tissue (NZO) by 5′RLM-RACE-PCR. With primers located in exon 3, we obtained 5′ sequences which markedly differed between both strains. The sequence of the B6 taste-bud mRNA was identical with that of the reference sequence (accession numbers: NM_008327, NM_011940). In contrast, the NZO-derived rapid amplification of cDNA-ends (RACE) product matched only partially to the reference sequence (exon 2), and appeared to be spliced to an alternative exon 1 (exon 1b). The variation in the genomic organization of the *Ifi202b* locus between B6 and NZO mice was confirmed by PCR on cDNA and genomic DNA. As shown in Figure 4, primers corresponding to the first exon of B6 in combination with reverse primers on exon 2 (P2) or 3 (P1) amplified a PCR product only on B6 DNA, while the same reverse primers (P3, P4) in combination with primers of the NZO-specific first exon generated a PCR product on NZO DNA. The PCR on the genomic DNA indicated that the first intron of B6 *Ifi202b* has a size of ~5 kb, that of NZO *Ifi202b* of 4 kb. Sequence analysis demonstrated that the homology between both intronic sequences stopped ~970 bp upstream of exon 2, indicating that B6 mice carry a microdeletion of the 5′-flanking region of *Ifi202b*, including its promoter, exon 1 and parts of the first intron. In taste buds, an alternative first exon (exon 1a) is spliced to exon 2,

Figure 3. Expression pattern of genes in the critical region of *Nob3*, including the *Ifi202b* cluster. (**A**) Expression of indicated genes was analysed in gonadal adipose tissue (upper panel) and skeletal muscle (lower panel) of B6.NZO-*Nob3.38*$^{B/B}$ and B6.NZO-*Nob3.38*$^{N/N}$ mice by qRT–PCR in pooled tissues from six mice per genotype (*N/N*, *B/B*) and normalized to *β-actin*. Expression was detected in duplicates and verified for the *Ifi200* cluster in skeletal muscle of six mice (see Supplementary Material, Fig. S2). *BC094916* and *1810030J14Rik* were not detectable; *EG666028* was not studied because no ESTs are listed in the databases. (**B**) Lack of expression of *Ifi202b* mRNA in tissues from parental B6 and NZO mice as determined by qRT–PCR ($n = 4–6$). Expression in taste buds (black bar) is driven by an alternative promoter and alternative exon 1 (Fig. 4). (**C**) Immunoreactive Ifi202b protein was detected in tissues of NZO but not in B6 mice by western blotting with antiserum raised against a peptide corresponding with the Ifi202b sequence (upper panel). Glyceraldehyde 3-phosphate dehydrogenase immunoreactivity was determined as loading control (lower panel). (**D**) Western blot analysis of lysates of skeletal muscle (quadriceps) of three individual B6.NZO-*Nob3.38*$^{B/B}$ and B6.NZO-*Nob3.38*$^{N/N}$ mice with the anti-Ifi202b antiserum.

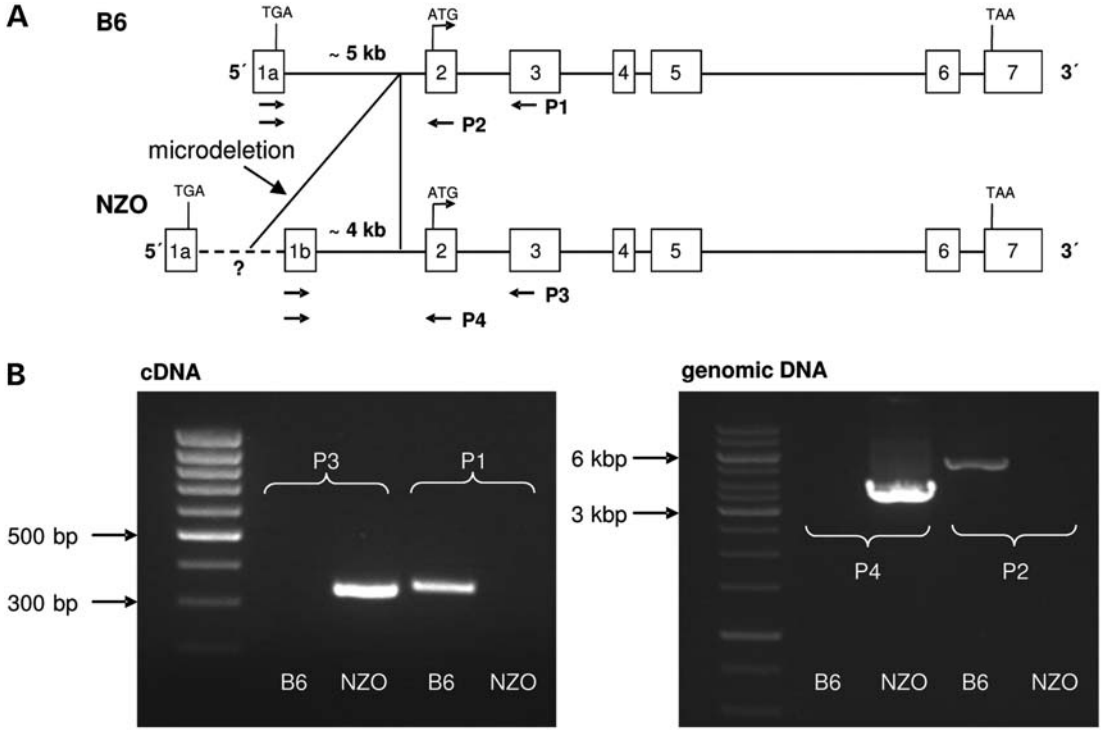

Figure 4. Microdeletion of exon 1 and the 5′-flanking region of the *Ifi202b* gene in B6. (**A**) Genomic organization and position of PCR primer pairs used for characterization of *Ifi202b* in B6 and NZO. (**B**) Identification of the variants in B6 and NZO by PCR with primers (P1–P4) as indicated in (A).

presumably driven by a different, taste-bud specific promoter (Fig. 4A). Interestingly, we can amplify the alternative exon 1a also on the genomic DNA of the NZO mouse (data not shown), indicating that the deletion in the B6 genome is located between the alternative exon 1a and the first intron of *Ifi202b* as indicated in Figure 4A.

Ifi202b affects the expression of other genes within the *Ifi200* cluster

It has been described previously that alterations in *Ifi200* expression result in the counterregulation of related *Ifi* transcripts (13–15). Thus, we tested whether the marked difference in *Ifi202b* expression is responsible for the increased expression of the other genes within this cluster (Fig. 3A). *Ifi202b* was overexpressed in muscle of B6 mice by electroporation of myc-tagged Ifi202b (Fig. 5A) and the expression of *Aim2, Pyhin1, Pydc3, Ifi204, Mndal, Ifi203* and *Ifi205* was determined. As expected, we detected a significantly lower expression of other *Ifi200* genes in muscles that were transfected with the cDNA of *Ifi202b* than in those transfected with a vector encoding green fluorescent protein (GFP; Fig. 5B). Overexpression of *Ifi202b* did not influence levels of *Pcp41l*, *Dusp23* and *Rgs5*, three transcripts located in close proximity of the *Ifi200* cluster but outside of the critical region (Fig. 5B).

Ifi202b modifies expression of *11β-Hsd1*

In order to identify a plausible biological mechanism linking *Ifi202b* expression in NZO mice with obesity, we studied the expression profiles of adipose tissues from B6.NZO-*Nob3.38*$^{B/B}$ and B6.NZO-*Nob3.38*$^{N/N}$ mice in detail and screened altered genes in respect to their impact on body weight and the metabolic syndrome. Table 1 shows a list of 11 genes with the strongest differences in expression between NZO- and B6-allele carriers. One important transcript which exhibits highly and significantly elevated expression in WAT of NZO-allele carrier is *11β-Hsd1* (Table 1, Fig. 6A). It drives lipid accumulation and adipocyte hypertrophy (16–19) as well as insulin resistance (20) when its expression is elevated. We confirmed the array data by qRT–PCR on WAT of B6.NZO-*Nob3.38*$^{B/B}$ and B6.NZO-*Nob3.38*$^{N/N}$ mice (Fig. 6B).

We next analyzed expression of *Ifi202b* in 3T3-L1 cells during differentiation. *Ifi202b* is expressed already in non-confluent 3T3-L1 fibroblasts. However, its levels increase 2-3 fold when cells reach confluence (preadipocytes) and differentiation is initiated until day 4 before they drop to initial levels at the stage of mature adipocytes at day 7 after initiation of differentiation (Fig. 7A, upper panel). In comparison, expression of *Pref1* (Fig. 7A, middle panel), an inhibitor of adipocyte differentiation was maximal in confluent preadipocytes and abolished during differentiation. We furthermore confirmed that *11β-Hsd1* expression is restricted to late stages of differentiation (20,21) (Fig. 7A, lower panel). Comparing *Ifi202b* and *11β-Hsd1* expression lead to the hypothesis that *Ifi202b* is required to induce *11β-Hsd1* expression. In order to test this, we suppressed *Ifi202b* in 3T3-L1 adipocytes by electroporating an *Ifi202b*-specific siRNA and determined mRNA levels of *11β-Hsd1*. As shown in Figure 7B, depletion of *Ifi202b* specifically suppressed *11β-Hsd1* expression and upregulated mRNA levels of *Pref1* (Fig. 7B). On the other

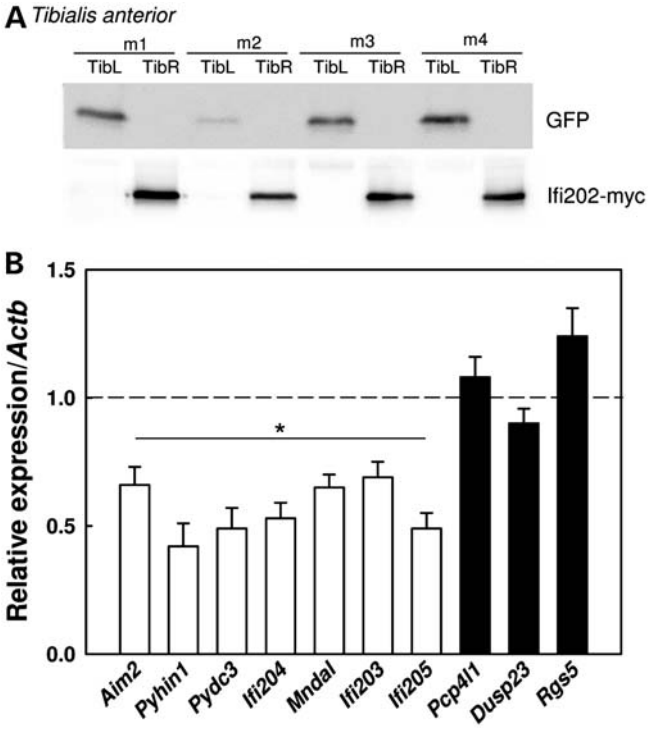

Figure 5. Overexpression of *Ifi202b* suppresses other genes within the *Ifi200* cluster. (**A**) A myc-tagged *Ifi202b* construct was transfected by IVE into the tibialis muscle of the right leg (TibR) of B6 mice; the left leg (TibL) was transfected with a GFP control plasmid and expression of Ifi202b and GFP was tested by western blotting. (**B**) Expression of the indicated transcripts was determined by qRT–PCR in tibialis muscles expressing *Ifi202b-myc*, and normalized for expression of β-actin. Black bars indicate expression levels of genes located in close proximity to the microdeletion but not belonging to the *Ifi200* cluster ($n = 12$) ($^*P < 0.0005$).

hand, *11β-Hsd1* mRNA levels increased after an adenovirus-mediated overexpression of *Ifi202b* (Fig. 7C). Similarly, overexpression of *Ifi202b* in tibialis muscle by electroporation increased *11β-Hsd1* expression (in Ifi202b transfected: 0.0113 ± 0.00065 versus GFP transfected control: 0.0097 ± 0.00061 level of expression in comparison to that of β-actin; $P = 0.0276$).

Altered mRNA levels of human *IFI* genes in white adipose tissue of obese individuals

In order to test whether the expression of *Ifi* genes is altered in human obesity, we determined their mRNA levels in visceral white adipose tissue of 53 lean (BMI < 25) and 221 obese (BMI > 30) individuals. The human syntenic region on Chr. 1 contains only four *Ifi* genes, *AIM2, IFI16*, *PYHIN* and *MNDA* (Fig. 8A). As illustrated in Figure 8B, mRNA levels of *IFI16* and *MNDA* were significantly higher in visceral adipose tissue of obese than in lean individuals (Fig. 8B). In addition, there was a significant correlation of maximal visceral fat cell size with *IFI16* ($r = 0.509$; $P = 0.002$) and *MNDA* mRNA ($r = 0.504$; $P = 0.002$). In contrast, mRNA levels of *PYHIN1* were significantly lower in adipose tissue of obese subjects (Fig. 8B).

Table 1. Genes with the strongest difference in expression as determined by expression profiling in white adipose tissue derived from the congenic line *Nob3.38*.

Gene symbol	Target id	log2 fold change	*P*-value
Ifi202b[a]	**NM_011940**	**12.52**	**5.1E−04**
Atp1a4	NM_013734	4.74	1.4E−02
ENSMUST00000111149	ENSMUST00000111149	2.98	6.1E−08
Hsd11b1	**NM_008288**	**2.47**	**3.2E−03**
Mucl1	NM_009268	1.83	1.8E−02
Ifi203[a]	**NM_001045481**	**−2.67**	**3.8E−05**
Ifi205[a]	**NM_172648**	**−2.84**	**3.9E−03**
ENSMUST00000160565	ENSMUST00000160565	−2.84	6.5E−04
AK014177	AK014177	−3.04	1.3E−03
Lefty1	NM_010094	−3.73	2.7E−07
AK079715	AK079715	−4.58	6.6E−05

$P \leq 0.05$ and log2 fold change ≥ 1.0 or ≤ -1.0. Genes with altered expression as verified by qRT-PCR are shown in bold.
[a]Genes located in critical fragment of *Nob3.38*.

DISCUSSION

The present data identify a microdeletion disrupting the transcriptional regulator Ifi202b on distal Chr. 1 of C57BL/6J mice as the most likely molecular cause for the anti-adipogenic effect of the B6 allele of mouse QTL *Nob3*. The following arguments lead to this conclusion: (i) with interval-specific congenics, we defined a critical genomic interval with 43 genes that were crucial to increase body weight. (ii) The most pronounced allelic variation was a microdeletion which includes the promoter and the first exon of *Ifi202b*. (iii) In NZO Ifi202b protein is most abundant in adipose tissue, and expression studies demonstrated a complete lack of its expression in B6 allele carriers. (iv) Suppression of *Ifi202b* expression in the congenic line as well as in cells transfected with siRNA decreased the levels of *11β-Hsd1*, which has previously been linked to visceral adiposity by direct evidence from transgenic and knockout mice. (v) Expression of the human *IFI* orthologues was affected in visceral adipose tissue of obese subjects.

Identification of *Ifi202b* as the causal gene crucially depends on exclusion of other sequence variations in the critical region in which we identified non-synonymous SNPs in several genes. First, *Ifi202b* was the only gene in the region exhibiting a significant differential expression in adipose tissue, liver and skeletal muscle associated with a structural variation. Secondly, except of *Spna1*—encoding for spectrin alpha 1—we failed to identify amino acid substitutions that are likely to alter protein function as classified by the Sift (Sorting intolerant from tolerant) program (22). Thirdly, we can exclude *Spna1* as responsible variant because its gene product is a major protein component of the red blood cell membrane skeleton (23) and its deficiency causes severe hereditary spherocytosis or hereditary elliptocytosis in mice (24), a phenotype not connected to obesity. However, we cannot entirely exclude that another gene in the critical region presumably together with *Ifi202b* participates in the induction of the adipogenic effect of *Nob3.38*.

The present data are the first to link the *Ifi202b* function with the regulation of energy balance and body weight. As a

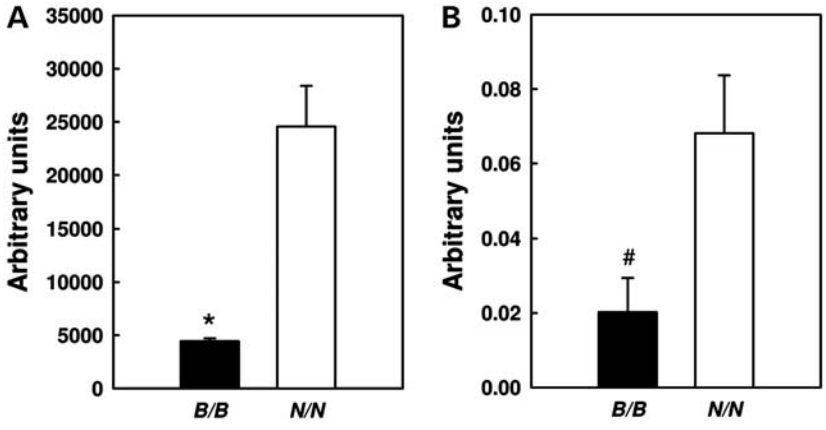

Figure 6. Expression of *11β-Hsd1* in white adipose tissue of NZO and B6 allele carriers. (**A**) Expression of *11β-Hsd1* in white adipose tissue of B6.NZO-*Nob3.38*$^{N/N}$ and B6.NZO-*Nob3.38*$^{B/B}$ mice ($n = 6$) as detected by array and (**B**) by qRT–PCR analysis ($^{\#}P < 0.05$; $^{*}P < 0.005$).

downstream target of *Ifi202b*, we identified *11β-Hsd1* by a transcriptome analysis of adipose tissue from B6.NZO-*Nob3.38*$^{B/B}$ and B6.NZO-*Nob3.38*$^{N/N}$ mice. Suppression and overexpression of *Ifi202b* expression in 3T3-L1 adipocytes provided direct evidence for a role of Ifi202b in the expression of *11β-Hsd1*. Furthermore, direct evidence linking *11β-Hsd1* expression with obesity has been published previously: mice lacking *11β-Hsd1* are protected against the development of obesity, whereas mice overexpressing *11β-Hsd1* in adipose tissues develop visceral adiposity and insulin resistance (16,18). Moreover, knockdown of *11β-Hsd1* in mice by antisense oligonucleotides protected against obesity by activating thermogenesis and increasing EE (25,26). This phenotype is consistent with that of B6 allele carriers of B6.NZO-*Nob3.38* mice which exhibited elevated EE presumably as a consequence of increased body temperature (12). The cortisone/cortisol system is not only involved in the stress response and inflammation but also in glucose and energy homeostasis. The enzyme 11β-Hsd1 mediates the conversion of cortisone (11-dehydrocorticosterone in rodents) to cortisol (corticosterone in rodents), locally within tissues. Thus, changes in the expression level of *11β-Hsd1* appear to contribute to altered glucocorticoid action in obesity especially when *11β-Hsd1* is elevated in adipose tissue (27).

That the presence of *Ifi202b* affects body weight is also visible in recombinant congenic lines of a C57BL/6 x DBA/2J cross (BXD; http://www.genenetwork.org). Lines carrying the DBA/2J fragment between 175.6 Mbp (determined by rs3682996) and 176.4 Mbp (rs3669108) including the *Ifi202b* locus and thereby the functional *Ifi202b* exhibited a higher body weight (18.5 ± 0.4 g) than those carrying the corresponding B6 allele (17.8 ± 0.35 g) (http://www.genenetwork.org); however, this difference is not significant ($P = 0.257$).

The *Ifi200* family encodes functionally related proteins described as transcriptional modulators. Increased expression of certain Ifi200 proteins in cells is associated with inhibition of cell proliferation, modulation of apoptosis and cell differentiation (28). Based on the finding that highest protein levels of *Ifi202b* were found in white adipose tissue, we suggest that this tissue plays an important role for the phenotype. In fact, *Ifi202b* is differentially expressed in 3T3-L1 cells with highest levels in the preadipocytes and early time points during differentiation, indicating that *Ifi202b* expression might be required for the induction of adipocyte-specific transcripts. However, the increased body weight of B6.NZO-*Nob3.38*$^{N/N}$ mice is not only associated with increased fat but also with elevated lean mass, indicating that either targets of *Ifi202b* other than *11β-Hsd1* or a gene other than *Ifi202b* might modulate lean mass.

The fact that human orthologues of *Ifi* exhibit an altered expression in visceral adipose tissue of obese subjects (Fig. 8) support the hypothesis that *Ifi* genes are somehow involved in adiposity and presumably in adipose tissue function. We detected higher expression of *IFI16* and *MNDA* in obese subjects, indicating that these two genes act in a related way to *Ifi202b* in the NZO mouse. Similar to the counter-regulatory effect of *Ifi202b* which influences expression of related transcripts, we observed that the increased expression of *IFI16* and *MNDA* in obese individuals is associated with the suppression of another *IFI* gene (*PYHIN1*). However, since there does not exist a direct orthologue for murine *Ifi202b* in humans, we only can speculate that alteration of human IFI transcripts participate in the obese phenotype. As expected, the human obesity gene map (2) shows several QTL on Chr. 1 for fat intake, abdominal subcutaneous fat and BMI. Specifically, QTL for waist circumference (LOD score 3.7) and the metabolic syndrome (LOD score of 4.5) defined by the markers *D1S1653-APOA2* and *D1S194-D1S196*, respectively, at chromosome 1q23.1–q23.2 are located in close proximity to the *IFI* genes (29).

We could prove the causal role of Ifi202b in the differential expression of the gene cluster by showing that overexpression of *Ifi202b* in skeletal muscle suppresses expression of related genes (Fig. 5), whereas *Ifi202b* depletion in 3T3-L1 adipocytes increased expression of *Ifi205*, *Mnda* and *If203* (data not shown).

In summary, our data present the identification of a microdeletion causing the disruption of *Ifi202b* in C57BL/6J mice which inhibits *11β-Hsd1* expression and presumably the activation of glucocorticoids in adipose tissue. It is suggested that these alterations protect from adiposity.

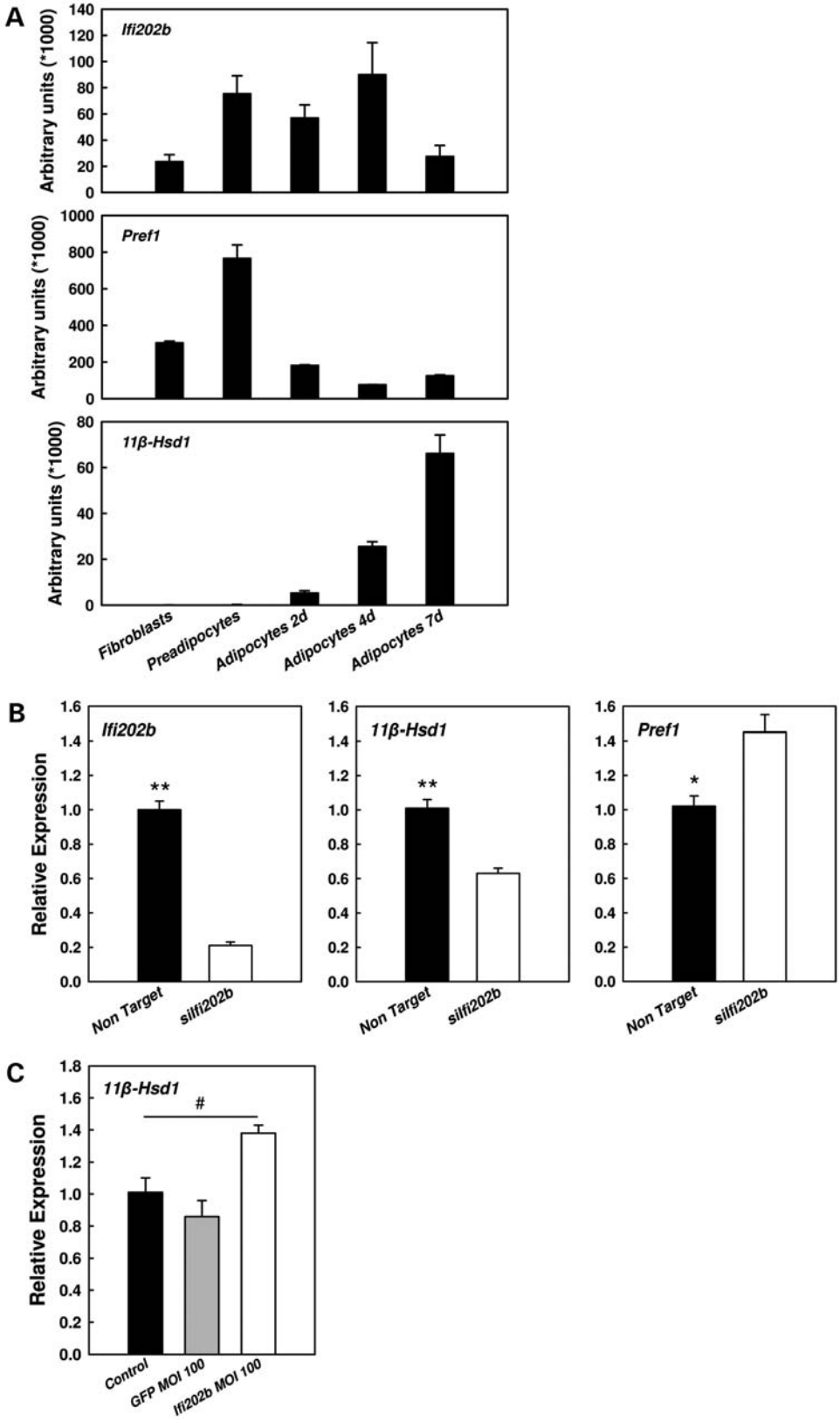

Figure 7. Expression pattern of selected genes in 3T3-L1 cells and effect of *Ifi202b* manipulation in 3T3-L1 adipocytes. (**A**) Expression of *Ifi202b* (upper panel), *Pref1* (middle panel) and *11β-Hsd1* mRNA (lower panel) in 3T3-L cells during differentiation ($n = 4$). (**B**) Suppression of *Ifi202b* in 3T3-L1 adipocytes by electroporation with an *Ifi202b*-specific siRNA ($n = 12$) and detection of *Ifi202b* (left panel), *11β-Hsd1* (middle panel) and *Pref1* (right panel) expression by qRT–PCR. (**C**) Overexpression of Ifi202b-myc (left panel) increases *11β-Hsd1* expression (right panel), while overexpression of GFP was without effect ($^{\#}P < 0.05$; $^{*}P < 0.005$; $^{**}P < 0.00005$).

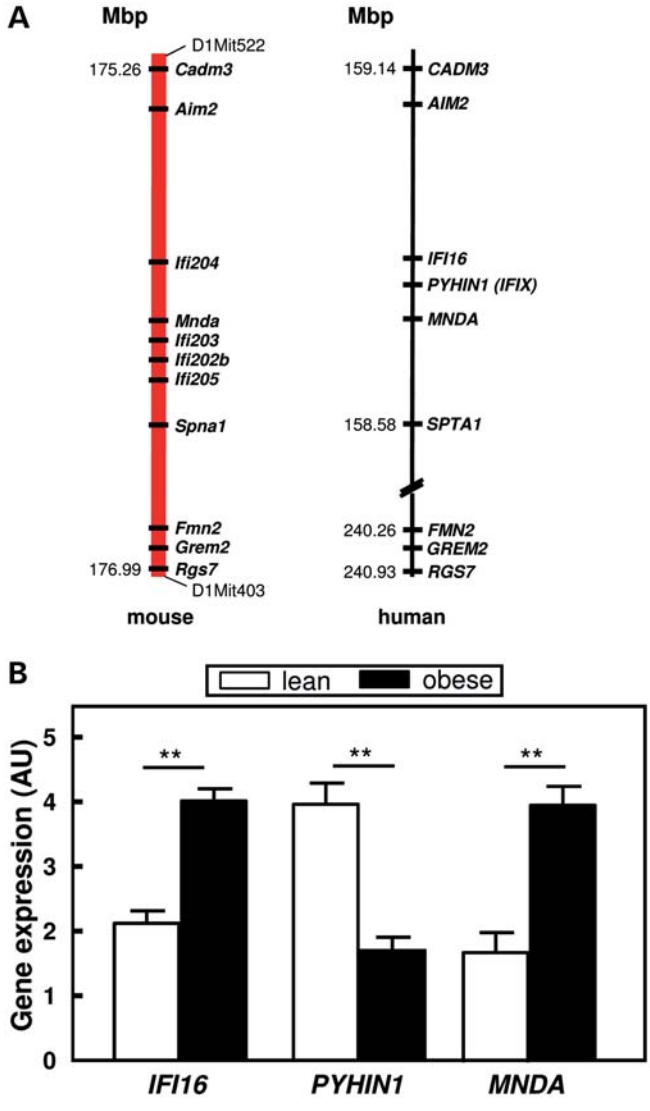

Figure 8. Expression of human *IFI* genes in adopose tissues. (**A**) Comparison of the *Ifi200* cluster with the syntenic region on human chromosome 1q23.1. (**B**) Expression of *IFI16*, *PYHIN1* and *MNDA* in adipose tissue of lean (BMI < 25 kg/m^2) and obese (BMI > 30 kg/m^2) human individuals. mRNA levels were determined by qRT–PCR in visceral adipose tissue from 53 controls and 221 obese individuals ($^*P < 0.05$; $^{**}P < 0.01$).

MATERIALS AND METHODS

Animals

The animals were kept in accordance with the NIH guidelines for the care and use of laboratory animals, and all experiments were approved by the ethics committee of the State Agency of Environment, Health and Consumer Protection (State of Brandenburg, Germany). Female NZO mice from our own colony (NZO/HIBomDife), C57BL/6J (Charles River, Sulzfeld, Germany) and congenic lines (12) were used throughout. Mice were housed at a temperature of 22°C with a 12:12 h light-dark cycle (lights on at 6:00 a.m.) in type II or type III macrolon cages with soft wood bedding. Standard chow (ssniff, Soest, Germany; maintenance diet for rats and mice, Art. No. V153xR/M-H) contained 19% (w/w) protein, 3.3% fat and 54.1% carbohydrates, with 26, 10 and 74% of total digestible energy (12.8 kJ/g) from protein, fat and carbohydrates, respectively. The high-fat diet (purified, Altromin, Lage, Germany; Art. No. C1057) contained (w/w) 18% protein, 15% fat and 46% carbohydrates, with 18, 35 and 47% of total digestible energy (16.2 kJ/g) from protein, fat and carbohydrates.

Breeding strategy and genotyping

Breeding of the congenic line B6.NZO-*Nob3.38* was previously described (12). Additional RCS were generated by backcrossing of male B6.NZO-*Nob3.38* with 6–12 B6 females. For genotyping, DNA was prepared from mouse tails with a DNA isolation kit based on a salt precipitation method (Invitek, Berlin, Germany) and used for tests with polymorphic microsatellite markers. Microsatellites were genotyped by PCR with oligonucleotide primers obtained from MWG (Ebersberg, Germany), and the microsatellite length was determined by non-denaturing polyacrylamide gel electrophoresis. For further fine mapping of the critical region, SNPs were used and analysed by sequencing.

Analysis of body composition

Body weights were measured with an electronic scale. Body fat and lean mass were determined with a nuclear magnetic resonance spectrometer (Bruker Minispec instrument, Echo Medical Systems, Houston, TX, USA) as described previously (30).

Indirect calorimetry

EE was measured at 22°C for 23 h with an open circuitry calorimetry system (Hartmann & Braun, Frankfurt/Main, Germany; VO_2 analyzer Magnos 16, VCO_2 analyzer Uras 14) as described previously (31,32). Air-tight respiratory cages with a flow rate of ~30 l/h were placed in climate chambers (Vötsch Industrietechnik, Reiskirchen-Lindenstruth, Germany) to maintain constant temperatures. Rate of oxygen consumption (VO_2) and rate of carbon dioxide production (VCO_2) were recorded in 6 min intervals for each animal, and EE was calculated with the equation $EE = 16.17VO_2 + 5.03VCO_2 + 5.98N$ (31,32), where EE is expressed in kilojoules per day, VO_2 and VCO_2 are expressed in liters per day. N is excreted nitrogen and was assumed to be 0.1 g/day. EE of each animal was calculated by dividing EE (kJ/day) by the lean mass of the animal and expressed as kilojoules per gram of lean mass per day.

Expression analysis in mouse tissues by expression profiling and quantitative real-time PCR

Total RNA from white adipose tissue, brown adipose tissue, hypothalamus, pituitary, taste buds enriched tissue and pancreas was extracted with the RNeasy Mini Kit (Qiagen, Hilden, Germany) according to the guidelines of the manufacturer. Extraction of total RNA from liver, skeletal muscle, testis and other tissues was performed with TRizol™ Reagent (Invitrogen, Carlsbad, CA, USA). First-strand cDNA synthesis was prepared with 2.0 μg total RNA,

random hexamer primer and SuperscriptIII reverse transcriptase (Invitrogen). Gene expression profiling was performed using 4 × 44 k Mouse Whole Genome Microarrays from Agilent Technologies. Quantitative real-time PCR was performed with an Applied Biosystems 7300 Real-time PCR system, with TaqMan Gene Expression Master Mix or Sybr-Green Master Mix (Applied Biosystems, Darmstadt, Germany), 25 ng cDNA and TaqMan Gene Expression Assays (Applied Biosystems) or oligonucleotides (MWG) (Supplementary Material, Table S3). Data were normalized referring to Livak and Schmittgen (33), whereas a β-actin expression assay was used as endogenous control.

Analysis of *MNDA*, *PYHIN1* and *IFI16* mRNA expression in human visceral adipose tissue

Samples of visceral adipose tissue were obtained from 438 Caucasian men ($N = 187$) and women ($N = 251$), who underwent abdominal surgery as described in detail elsewhere (34). The age ranged from 16 to 82 years and BMI from 17.6 to 119 kg/m^2. In these subjects, abdominal visceral fat area was calculated using abdominal MRI scans or computed tomography scans at the level of L4–L5. Percentage body fat was measured by dual-energy X-ray absorptiometry (DEXA). Individuals fulfilled the following exclusion criteria: (i) any acute or chronic inflammatory disease as determined by a leucocyte count > 7000 Gpt/l, C-reactive protein > 5.0 mg/dl or clinical signs of infection, (ii) detectable antibodies against glutamic acid decarboxylase, (iii) medical history of hypertension, i.e. systolic blood pressure was <140 mmHg and diastolic blood pressure was <85 mmHg, (iv) clinical evidence of either cardiovascular or peripheral artery disease, (v) thyroid dysfunction, (vi) alcohol or drug abuse and (vii) pregnancy. All subjects had a stable weight with fluctuations smaller than 2% of the body weight for at least 3 months before surgery. The study was approved by the ethics committee of the University of Leipzig. All subjects gave written informed consent before taking part in the study.

Total RNA was isolated from omental adipose tissue samples using TRizol (Life Technologies, Grand Island, NY, USA), and 1 μg RNA was reverse transcribed with standard reagents (Life Technologies). *MNDA* (Hs00935905_m1), *PYHIN1* (Hs00378651_m1) and *IFI16* (Hs00194261_m1) mRNA expression levels were determined by premixed assays. Samples were incubated in the ABI PRISM 7000 sequence detector for an initial denaturation at 95°C for 10 min, followed by 40 PCR cycles, each cycle consisting of 95°C for 15 s, 60°C for 1 min and 72°C for 1 min. *MNDA, PYHIN1* and *IFI16* mRNA expression was calculated relative to the mRNA expression of *18S rRNA*, determined by a premixed assay on demand for human *18S rRNA* (Applied Biosystems).

RACE PCR

Rapid amplification of cDNA ends for determination of 5′ends was performed with the FirstChoice RLM-RACE Kit (Ambion, Darmstadt, Germany) according to the manufacturers' instructions.

Sequencing

Sequence analysis of genes located in the critical region was done with the sequence capture technology based on the procedure described in reference (35). Sequencing of DNA was performed with a 3130xl Genetic Analyzer (Applied Biosystems) in combination with the BigDye Terminator v3.1 Cycle Sequencing Kit (Applied Biosystems). Sequence analysis was done by SeqScape software 2.5 (Applied Biosystems).

Antibodies and western blotting

For the specific detection of Ifi202b, we raised a polyclonal antiserum in guinea pig against two specific peptides (1–20: MSNRNLRSSTNSEFSEGQHQ and 336–349: KSQNKEDS SSSDER), performed an affinity purification of the serum and used it in a dilution of 1:50 for western blotting. The anti-glyceraldehyde 3-phosphate dehydrogenase antibody was purchased from Ambion (Austin, TX, USA) and used in a dilution of 1:8000 as loading control in western blots.

siRNA-mediated knockdown of *Ifi202b* in 3T3-L1 cells

For suppression of *Ifi202b*, 3T3-L1 fibroblasts (5 × 10^4 cells/electroporation) and adipocytes (7 × 10^3 cells/electroporation) were electroporated with the Bio-Rad Gene Pulser II with settings of 170 V and 950 μF with 4 nmol *Ifi202b*-specific small interfering RNA (siRNA) (Mm_Ifi202b_2: 5′-AAAGAUAAU GAAGAUAAUAUAUU-3′, Thermo Scientific Dharmacon). For control experiments, cells were electroporated with 4 nmol non-target siRNA (5′-UAGCGACUAAACACAUCA AUU-3′, Thermo Scientific Dharmacon). After electroporation, cells were immediately mixed with fresh medium before being reseeded onto six-well plates. RNA was isolated 48 h after electroporation.

Overexpression of Ifi202 in 3T3-L1 adipocytes

The cDNA of Ifi202b-myc was subcloned into an adenovirus (VQAd; ViraQuest, Inc., North Liberty, IA, USA). For overexpression, VQAd-Ifi202b-myc with MOI of 100 was preincubated with 0.5 mg/ml poly-L-lysine in IMDM plus 0.5% BSA at room temperature for 100 min. Cells were washed with phosphate buffered saline (PBS) and incubated with the virus at 37°C for 100 min before adding equivalent amount of IMDM/0.5% BSA for an overnight incubation. Cells were washed twice with PBS and cultured with IMDM/10% FBS for additional 72 h before harvest. As a control cells were transfected with a GFP encoding adenovirus.

Overexpression of Ifi202b in tibialis anterior

In vivo electroporation (IVE) was performed as described previously (36). In brief, plasmids were purified using Endotoxin-free Mega-Prep kits (Qiagen), and resuspended in sterile 0.9% saline. Animals to be electroporated were anesthetized with isofluran and their hindlimbs shaved. *Tibialis anterior* (TA) muscles were injected with 15 units of hyaluronidase using an insulin syringe. After 60 min, animals were anesthetized

again and 15 μg of Ifi202b expression plasmid (pCMV-myc-Ifi202b) in 30 μl saline was injected in the TA muscle. The contralateral muscle received injection with pEGFP vector as internal control. This was immediately followed by the application of a pair of tweezer electrodes (BTX) across the distal limb connected to an ECM-830 electroporator device (BTX). Application of eight 20 ms pulses of 80 V at a frequency of 1 Hz was used to facilitate plasmid uptake. Animals were sacrificed 7 days later and muscle rapidly dissected and shock frozen in liquid nitrogen.

Statistical analysis

Values are reported as means ± SE, unless otherwise noted. Differences between *B/B* and *N/N* genotypes were tested by two-tailed Student's *t*-test. Statistical analysis for more than two groups was performed using two-way analysis of variance and *post hoc* with Scheffe's test (Statview Program, SAS Institute, Inc., Cary, NC, USA). Expression levels determined by quantitative real-time PCR were compared by the nonparametric Kruskal–Wallis *H*-test. A *P*-value <0.05 ($P < 0.05$) was considered significant.

SUPPLEMENTARY MATERIAL

Supplementary Material is available at *HMG* online.

ACKNOWLEDGEMENTS

We thank Alan Attie for giving us access to unpublished data and for many helpful comments. The authors are indebted to Michaela Rath, Monika Niehaus, Malte Neubauer and Neele Gerhardt for expert technical assistance, and Vera Bartsch for data analysis.

Conflict of Interest statement. None declared.

FUNDING

This work was supported by the German Ministry of Education and Research (NGFN2: 01GS0487; NGFNplus: 01GS0821; NEUROTARGET: 01GI0847; DZD: 01GI0922).

REFERENCES

1. Lander, E. and Kruglyak, L. (1995) Genetic dissection of complex traits: guidelines for interpreting and reporting linkage results. *Nat. Genet.*, **11**, 241–247.
2. Rankinen, T., Zuberi, A., Chagnon, Y.C., Weisnagel, S.J., Argyropoulos, G., Walts, B., Pérusse, L. and Bouchard, C. (2006) The human obesity gene map: the 2005 update. *Obesity (Silver Spring)*, **14**, 529–644.
3. Frayling, T.M., Timpson, N.J., Weedon, M.N., Zeggini, E., Freathy, R.M., Lindgren, C.M., Perry, J.R., Elliott, K.S., Lango, H., Rayner, N.W. *et al.* (2007) A common variant in the *FTO* gene is associated with body mass index and predisposes to childhood and adult obesity. *Science*, **316**, 889–894.
4. Dina, C., Meyre, D., Gallina, S., Durand, E., Körner, A., Jacobson, P., Carlsson, L.M., Kiess, W., Vatin, V., Lecoeur, C., Delplanque, J. *et al.* (2007) Variation in *FTO* contributes to childhood obesity and severe adult obesity. *Nat. Genet.*, **39**, 724–726.
5. Willer, C.J., Speliotes, E.K., Loos, R.J., Li, S., Lindgren, C.M., Heid, I.M., Berndt, S.I., Elliott, A.L., Jackson, A.U., Lamina, C., Lettre, G. *et al.* (2009) Six new loci associated with body mass index highlight a neuronal influence on body weight regulation. *Nat. Genet.*, **41**, 25–34.
6. Thorleifsson, G., Walters, G.B., Gudbjartsson, D.F., Steinthorsdottir, V., Sulem, P., Helgadottir, A., Styrkarsdottir, U., Gretarsdottir, S., Thorlacius, S., Jonsdottir, I., Jonsdottir, T. *et al.* (2009) Genome-wide association yields new sequence variants at seven loci that associate with measures of obesity. *Nat. Genet.*, **41**, 18–24.
7. Bessesen, D.H. (2008) Update on obesity. *J. Clin. Endocrinol. Metab.*, **93**, 2027–2034.
8. Jürgens, H.S., Schürmann, A., Kluge, R., Ortmann, S., Klaus, S., Joost, H.G. and Tschop, M.H. (2006) Hyperphagia, lower body temperature, and reduced running wheel activity precede development of morbid obesity in New Zealand obese mice. *Physiol. Genomics*, **25**, 234–241.
9. Ortlepp, J.R., Kluge, R., Giesen, K., Plum, L., Radke, P., Hanrath, P. and Joost, H.G. (2000) A metabolic syndrome of hypertension, hyperinsulinaemia and hypercholesterolaemia in the New Zealand obese mouse. *Eur. J. Clin. Invest.*, **30**, 195–202.
10. Chadt, A., Leicht, K., Deshmukh, A., Jiang, L.Q., Scherneck, S., Bernhardt, U., Dreja, T., Vogel, H., Schmolz, K., Kluge, R., Zierath, J.R. *et al.* (2008) Tbc1d1 mutation in lean mouse strain confers leanness and protects from diet-induced obesity. *Nat. Genet.*, **40**, 1354–1359.
11. Scherneck, S., Nestler, M., Vogel, H., Blüher, M., Block, M.D., Diaz, M.B., Herzig, S., Schulz, N., Teichert, M., Tischer, S., Al-Hasani, H. *et al.* (2009) Positional cloning of zinc finger domain transcription factor Zfp69, a candidate gene for obesity-associated diabetes contributed by mouse locus Nidd/SJL. *PLoS Genet.*, **5**, e1000541.
12. Vogel, H., Nestler, M., Rüschendorf, F., Block, M.D., Tischer, S., Kluge, R., Schürmann, A., Joost, H.G. and Scherneck, S. (2009) Characterization of Nob3, a major quantitative trait locus for obesity and hyperglycaemia on mouse chromosome 1. *Physiol. Genomics*, **38**, 226–232.
13. Gribaudo, G., Riera, L., De Andrea, M. and Landolfo, S. (1999) The antiproliferative activity of the murine interferon-inducible Ifi 200 proteins depends on the presence of two 200 amino acid domains. *FEBS Lett.*, **456**, 31–36.
14. Rozzo, S.J., Allard, J.D., Choubey, D., Vyse, T.J., Izui, S., Peltz, G. and Kotzin, B.L. (2001) Evidence for an interferon-inducible gene, Ifi202, in the susceptibility to systemic lupus. *Immunity*, **15**, 435–443.
15. Panchanathan, R., Duan, X., Shen, H., Rathinam, V.A., Erickson, L.D., Fitzgerald, K.A. and Choubey, D. (2010) Aim2 deficiency stimulates the expression of IFN-inducible Ifi202, a lupus susceptibility murine gene within the Nba2 autoimmune susceptibility locus. *J. Immunol.*, **185**, 7385–7393.
16. Masuzaki, H., Paterson, J., Shinyama, H., Morton, N.M., Mullins, J.J., Seckl, J.R. and Flier, J.S. (2001) A transgenic model of visceral obesity and the metabolic syndrome. *Science*, **294**, 2166–2170.
17. De Sousa Peixoto, R.A., Turban, S., Battle, J.H., Chapman, K.E., Seckl, J.R. and Morton, N.M. (2008) Preadipocyte 11beta-hydroxysteroid dehydrogenase type 1 is a keto-reductase and contributes to diet-induced visceral obesity in vivo. *Endocrinology*, **149**, 1861–1868.
18. Kannisto, K., Pietiläinen, K.H., Ehrenborg, E., Rissanen, A., Kaprio, J., Hamsten, A. and Yki-Järvinen, H. (2004) Overexpression of 11beta-hydroxysteroid dehydrogenase-1 in adipose tissue is associated with acquired obesity and features of insulin resistance: studies in young adult monozygotic twins. *J. Clin. Endocrinol. Metab.*, **89**, 4414–4421.
19. Michailidou, Z., Jensen, M.D., Dumesic, D.A., Chapman, K.E., Seckl, J.R., Walker, B.R. and Morton, N.M. (2007) Omental 11beta-hydroxysteroid dehydrogenase 1 correlates with fat cell size independently of obesity. *Obesity (Silver Spring)*, **15**, 1155–1163.
20. Morton, N.M., Paterson, J.M., Masuzaki, H., Holmes, M.C., Staels, B., Fievet, C., Walker, B.R., Flier, J.S., Mullins, J.J. and Seckl, J.R. (2004) Novel adipose tissue-mediated resistance to diet-induced visceral obesity in 11 beta-hydroxysteroid dehydrogenase type 1-deficient mice. *Diabetes*, **53**, 931–938.
21. Napolitano, A., Voice, M.W., Edwards, C.R., Seckl, J.R. and Chapman, K.E. (1998) 11Beta-hydroxysteroid dehydrogenase 1 in adipocytes: expression is differentiation-dependent and hormonally regulated. *J. Steroid Biochem. Mol. Biol.*, **64**, 251–260.
22. Ng, P.C. and Henikoff, S. (2001) Predicting deleterious amino acid substitutions. *Genome Res.*, **11**, 863–874.
23. Wandersee, N.J., Birkenmeier, C.S., Gifford, E.J., Mohandas, N. and Barker, J.E. (2000) Murine recessive hereditary spherocytosis, sph/sph, is caused by a mutation in the erythroid alpha-spectrin gene. *Hematol. J.*, **1**, 235–242.

24. Wandersee, N.J., Birkenmeier, C.S., Bodine, D.M., Mohandas, N. and Barker, J.E. (2003) Mutations in the murine erythroid alpha-spectrin gene alter spectrin mRNA and protein levels and spectrin incorporation into the red blood cell membrane skeleton. *Blood*, **101**, 325–330.
25. Hermanowski-Vosatka, A., Balkovec, J.M., Cheng, K., Chen, H.Y., Hernandez, M., Koo, G.C., Le Grand, C.B., Li, Z., Metzger, J.M., Mundt, S.S. *et al.* (2005) 11beta-HSD1 inhibition ameliorates metabolic syndrome and prevents progression of atherosclerosis in mice. *J. Exp. Med.*, **202**, 517–527.
26. Li, G., Hernandez-Ono, A., Crooke, R.M., Graham, M.J. and Ginsberg, H.N. (2011) Antisense reduction of 11β-hydroxysteroid dehydrogenase type 1 enhances energy expenditure and insulin sensitivity independent of food intake in C57BL/6J mice on a Western-type diet. *Metabolism*, [Epub ahead of print].
27. Mortion, N.M. and Seckl, J.R. (2008) 11β-hydroxysteroid dehydrogenase type 1 and obesity. In *Obesity and Metabolism; Frontiers of Human Research*. Karger, London, Vol. 36.
28. Choubey, D. and Panchanathan, R. (2008) Interferon-inducible Ifi200-family genes in systemic lupus erythematosus. *Immunol. Lett.*, **119**, 32–41.
29. Ng, M.C., So, W.Y., Lam, V.K., Cockram, C.S., Bell, G.I., Cox, N.J. and Chan, J.C. (2004) Genome-wide scan for metabolic syndrome and related quantitative traits in Hong Kong Chinese and confirmation of a susceptibility locus on chromosome 1q21-q25. *Diabetes*, **53**, 2676–2683.
30. Buchmann, J., Meyer, C., Neschen, S., Augustin, R., Schmolz, K., Kluge, R., Al-Hasani, H., Jürgens, H., Eulenberg, K., Wehr, R., Dohrmann, C. *et al.* (2007) Ablation of the cholesterol transporter adenosine triphosphate-binding cassette transporter G1 reduces adipose cell size and protects against diet-induced obesity. *Endocrinology*, **148**, 1561–1573.
31. Klaus, S., Rudolph, B., Dohrmann, C. and Wehr, R. (2005) Expression of uncoupling protein 1 in skeletal muscle decreases muscle energy efficiency and affects thermoregulation and substrate oxidation. *Physiol. Genomics*, **21**, 193–200.
32. Frenz, U. (1999) Whole body calorimetry. In Kemp, R.B. (ed.), *Handbook of Thermal Analysis and Calorimetry. Vol. 4: From Macromolecules to Man*. Elsevier, Amsterdam, New York, Tokyo, pp. 511–555.
33. Livak, K.J. and Schmittgen, T.D. (2001) Analysis of relative gene expression data using real-time quantitative PCR and the 2(-Delta Delta C(T)) method. *Methods*, **25**, 402–408.
34. Berndt, J., Klöting, N., Kralisch, S., Kovacs, P., Fasshauer, M., Schon, M.R., Stumvoll, M. and Blüher, M. (2005) Plasma visfatin concentrations and fat depot-specific mRNA expression in humans. *Diabetes*, **54**, 2911–2916.
35. Hodges, E., Rooks, M., Xuan, Z., Bhattacharjee, A., Benjamin Gordon, D., Brizuela, L., Richard McCombie, W. and Hannon, G.J. (2009) Hybrid selection of discrete genomic intervals on customdesigned microarrays for massively parallel sequencing. *Nat. Protoc.*, **4**, 960–974.
36. Kanzleiter, T., Preston, E., Wilks, D., Ho, B., Benrick, A., Reznick, J., Heilbronn, L.K., Turner, N. and Cooney, G.J. (2010) Overexpression of the orphan receptor Nur77 alters glucose metabolism in rat muscle cells and rat muscle in vivo. *Diabetologia*, **53**, 1174–1183.